Supplementary Materials for

Complement and microglia mediate early synapse loss in Alzheimer mouse models

Soyon Hong, Victoria F Beja-Glasser†, Bianca M Nfonoyim†, Arnaud Frouin, Shaomin Li, Saranya Ramakrishnan, Katherine M Merry, Qiaoqiao Shi, Arnon Rosenthal, Ben A Barres, Cynthia A Lemere, Dennis J Selkoe and Beth Stevens*

*Email correspondence to: beth.stevens@childrens.harvard.edu
† These authors contributed equally.

This PDF file includes:

Materials and Methods
Figs. S1 to S12

Materials and Methods

Animals

All experiments were reviewed and overseen by the institutional animal use and care committee in accordance with all NIH guidelines for the humane treatment of animals. J20 (C57BL6xDBA2 background), *C1qa* KO (C57BL6 background), and Homer-GFP (C57BL6 background) lines were kind gifts from L. Mucke, M. Botto, and S. Okabe, respectively, and were maintained in our breeding colony. All WT mice used in this study were sex-matched littermate controls on C57BL6 background unless otherwise specified. *CR3* KO mice were originally obtained from Jackson Labs and maintained in our breeding colony. For APP/PS1x*C3* KO studies, the individual APP/PS1 and *C3* KO lines were originally obtained from Jackson Labs. *C3* KO mice were first bred to APP/PS1 mice, then to APPX*C3* hets, and finally, to APPx*C3* KO mice to generate APP/PS1x*C3* KO vs. *C3* KO littermates.

Antibodies

For complement immunohistochemistry antibodies, C1q (in-house (*13*) but now available at Abcam ab182451) and C3 (Cappel 55730) were used. For C1q function blocking antibody (Figs. 3B and C), ANX-M1 from Annexon Biosciences was used. See below for details on ANX-M1 C1q antibody production and *in vitro* characterization. For synaptic antibodies, PSD95 (Millipore MAB1596), synaptophysin (Abcam ab16659), and homer, synaptotagmin and synapsin (Synaptic Systems 160-011, 105-002 and 106-103, respectively) were used. For antibodies against microglia/macrophages, Iba1 (Wako 019-19741), CD11b (Serotec MCA711G), CD68 (Serotec MCA1957) and P2RY12 (kind gift of O. Butovsky, BWH (*22*)) were used. 3D6 (Elan, plc (*26*)) was used to stain humanized $A\beta_{1-5}$.

Aβ Sources and Characterization

As the Aβ monomer source, we used $A\beta_{1-40}$ monomers (MesoScale Discovery), and for the Aβ oligomer-rich source, we used the disulfide-crosslinked $(A\beta_{1-40}\ S26C)_2$ oligomers (kind gift of D. Walsh (BWH)). We defined Aβ oligomers similar to Hong et al. (*26*): as soluble low molecular weight oligomers (dimers, trimers, tetramers, etc.) that remain in the supernatant after high speed ultracentrifugation, as opposed to high molecular weight, prefibrillar Aβ aggregates that can often be pelleted by ultracentrifugation. Care was taken to avoid freeze-thaw of the Aβ monomers and S26C oligomers, and their monomeric and oligomeric states were confirmed using Western blotting and Aβ oligomer-specific ELISAs as previously described (*26*).

ANX-M1 C1q neutralization antibody production and *in vitro* characterization

The ANX-M1 C1q function blocking antibody (Annexon Biosciences) was generated by immunizing *C1qa* KO mice with human C1q protein purified from human plasma (Complement Technology Inc. Tyler Texas, Cat #A-099) using standard mouse immunization and hybridoma screening technologies. In brief, mice were intraperitoneally (IP) injected with 25 μg of human C1q protein in complete Freund's adjuvant (CFA) on Day 0 and boosts were done with 25 μg of C1q enzyme in incomplete

Freund's adjuvant (IFA) on days 21, 42, 52, and a final intravenous boost on Day 63. 4 d following the final boost the mice were euthanized, spleens were removed and splenocytes were fused with the myeloma cell line SP2/0. Fused cells were grown on hypoxanthine-aminopterin-thymidine (HAT) selective semisolid media for 10-12 d and the resulting hybridoma clones were transferred to 96-well tissue culture plates and grown in HAT medium until the antibody titer was high. The antibody-rich supernatants of the clones were isolated and tested for reactivity with C1q.

C1q-antibody interactions were measured using an OCTET™ System according to standard protocols and manufacturer's instructions. Briefly, human and mouse C1q proteins were immobilized separately on a biosensor at three concentrations (3 nM, 1.0 nM, and 0.33 nM). Next, the anti-C1q antibody was injected onto the C1q-coated biosensor at a concentration of 2.0 g/ml and the association constants (kon) and dissociation constants (kQff) for anti-C1q antibodies were measured. The data were fit by non-linear regression analysis and using the Octet Data Analysis software to yield affinity (KD) and kinetic parameters (kon/off) for the interactions of the antibody with human ($1.28x10^{11}$) and mouse ($3.23x10^{11}$) C1q respectively.

Anti-C1q antibodies were tested in human and rodent hemolytic assays (CH50) for their ability to neutralize C1q and block its activation of the downstream complement cascade. CH50 assays were conducted essentially as described in Current Protocols in Immunology (1994) Supplement 9 Unit 13.1. In brief, 5 µl of human serum (Cedarlane, Burlington, NC), 0.625 µl of Wistar rat serum, or 2.5 µl of C57B1/6 mouse serum was diluted to 50 µl of GVB buffer (Cedarlane, Burlington, NC) and added to 50 µl of the monoclonal antibodies (1 µg) diluted in GVB buffer. The antibody: serum mixture was pre-incubated for 30 min on ice, then added to 100 µl of EA cells (2x10 /ml) for rat and human assays and 4x107 ml for mouse assays. The EA cells were generated exactly as specified in Current Protocols using Sheeps blood in Alsever's (Cedarlane Cat #CL2581) and hemolysin (Cedalane Cat #CL9000). The EA cells, serum and antibody mixture was incubated for 30 minutes at 37°C, then placed on ice. Next, 1.2 ml of 0.15 M NaCl was added to the mixture and the OD_{412} of the sample was read in a spectrophotometer to determine the amount of cell lysis. The percent inhibition of the test antibodies was determined relative to a control mouse IgGl antibody (Abcam ab 18447). The Anti-C1q antibody was tested for its C1q neutralizing activity in human, mouse, and rat CH50 assays. Testing was conducted in dose-response formats. M1 was demonstrated to neutralize C1q activity in human, mouse, and rat CH50 hemolysis assays in a dose-dependent manner. In the human and rat CH50 hemolysis assays, M1 inhibited greater than 90% and up to 100% of hemolysis. In the mouse assay, M1 inhibited greater than 50% of hemolysis. In the mouse CH50 assay, approximately 500 ng of M1 was required to achieve 50% inhibition of hemolysis. In the rat CH50 assay, less than 16 ng was required to achieve 50% inhibition of hemolysis.

Immunohistochemistry and microscopy

For immunohistochemical analyses and imaging using confocal and SIM techniques, similar protocols were modified (*6, 10, 26*). Briefly, mice were perfused with PBS followed by 4% PFA (Electron Microscopy Sciences 15710) and brains were postfixed for 2 h at 4°C, transferred to 30% sucrose for 24-48 h then embedded for cryostat sectioning. 14-µm thick cryosections were permeabilized at RT either in 5% BSA and

0.2% Triton-X 100 (Sigma, A2153 and T8787 respectively) for 1 h or in 10% Normal Goat Serum (Sigma G9023) and 0.3% Triton X-100 for 2 h, followed by primary antibody overnight at 4°C. For microglial engulfment assays, 40-µm thick cryosections were used and permeabilized at RT in 5% BSA and 1% Triton-X 100. Sections were then treated with the appropriate Alexa-fluorophore-conjugated secondary antibodies and mounted with vectashield containing DAPI (Vector labs H-1000). For confocal, all images were acquired using LSM700 confocal microscope and Zen 2009 image acquisition software (Carl Zeiss), and ImageJ was used to perform background subtraction and thresholding. For microglial engulfment assays, background subtraction was performed using ImageJ, then Imaris software was used to perform 3D reconstruction and surface rendering (*6, 19*). For acquiring, processing and analyzing SIM images, a similar protocol in Hong et al. was followed (*10*). Briefly, immunohistochemistry was performed on 14-µm thick cryosections following the protocol mentioned above, then Hoescht (0.01%, Life technologies H3570) was added to appropriate Alexa-fluorophore-conjugated secondary antibodies and mounted with Prolong Gold (Invitrogen P36934). All samples were imaged using a Zeiss ELYRA PS1 microscope with a fixed number of grating rotations (5) and images were processed using the accompanied Zen image acquisition software (Carl Zeiss). Then, the processed 3D SIM images were analyzed using Imaris using the spot (ellipsoids) function, and MatLab was used to determine the number of colocalized (≤ 200 nm distance between spot centers of two synaptic channels) spots. Number of colocalized spots was then divided by total volume of the image stack.

Electron Microscopy (EM) and Analysis

Animals were perfused with 2.5% Glutaraldehyde (Ted Pella 18420)/2% Paraformaldehyde (Ted Pella 18501) in 0.1 M sodium cacodylate buffer (pH 7.4) (Ted Pella 18851). The hippocampus was dissected out, sliced into 1 mm slices, washed in 0.1 M cacodylate buffer and postfixed with 1% Osmiumtetroxide (OsO_4) (Ted Pella 18459) /1.5% Potassiumferrocyanide ($KFeCN_6$) (Electron Microscopy Sciences 20150) for 1 h, washed in water 3x and incubated in 1% aqueous uranyl acetate for 1 h followed by 2 washes in water and subsequent dehydration in grades of alcohol (10 min each; 50%, 70%, 90%, 2x 10 min 100%). The samples were then placed in propyleneoxide for 1 h subsequently infiltrated overnight in a 1:1 mixture of propyleneoxide and TAAB Epon (Marivac Canada Inc. St. Laurent, Canada). The following day the samples were embedded in TAAB Epon and polymerized at 60°C for 48 h.

Ultrathin sections (about 60 nm) were cut on a Reichert Ultracut-S microtome, placed onto copper grids, stained with uranyl acetate and lead citrate and examined in a TecnaiG² Spirit BioTWIN. Images were recorded with an AMT 2k CCD camera. Fifteen distinct apical regions (stratum radiatum) of CA1, ~50-100 µM from the cellbody layer of the hippocampus were imaged per animal. Images were used to analyze the number of synapses blind to the genotype. A synapse was defined as an electron dense post-synaptic density areas juxtaposed to presynaptic terminals filled with synaptic vesicles.

Compound E Treatment

1 mo J20 mice or their sex-matched littermate controls received IP injections of Compound E (3 mg/kg, Axxora BV-1949) or DMSO control diluted in 1:1

PBS:Propylene glycol for three times total every 5 h. Half-lives were calculated according to previous studies using *in vivo* microdialysis and brain homogenates (*12, 26*). Post 5 h after the third injection, brains were harvested for immunohistochemistry.

Intracerebroventricular (ICV) or tail vein injections of Aβ

For ICV injection (Figs. 2, 3A, 4A and 4B, S5, S6, S8, S10, and S11), Aβ monomers, Aβ oligomers (1-5 ng; volume 1-5 µl) or PBS (volume 1-5 µl) were stereotaxically injected into left lateral ventricles (-0.4 mm anteroposterior, 1 mm mediolateral and -2.5 mm dorsoventral) via a Hamilton syringe at 0.5 µl/min in young adult (3 mo) anesthetized mice following a similar protocol previously described (*26*). Upon completion of injection (< 15 min), mice were allowed to wake up from anesthesia. 18 or 72 h after ICV injection, brains were harvested for immunohistochemistry. For tail vein injection experiments pertaining to CR3 (Figs. 4C and 4D), 100 ng (volume 100 µl) of Aβ oligomers or PBS (volume 100 µl) was delivered using sterile 30 ½ needle in a 1 ml syringe. Mice were sacrificed for immunohistochemistry 18 or 72 h post injection. No gross toxic effect, overt sign of distress or pain, or any other behavioral changes was observed as expected with either ICV or tail vein injection procedure.

ICV injection of Aβ and ANX-M1 C1q antibody

For the C1q neutralizing experiment (Figs. 3B and S8B), 3 mo WT mice first received IP injections of either the ANX-M1 C1q function blocking antibody (Annexon Biosciences) or IgG isotype control (Annexon Biosciences or *InVivoMAb*) 20 mg/kg. 15 min following the IP injections, mice underwent anesthesia to receive ICV injections of first, the C1q antibody or IgG control (5 µg), then ~2 min after, PBS or Aβ oligomers (5 ng). Mice were allowed to promptly recover and were given additional IP injections of C1q antibody or IgG control (20 mg/kg) 24 h and 48 h following the initial IP injections (*i.e.*, total 3 IP injections). Brains were then harvested at 72 h for immunohistochemistry analysis.

LTP induction on acute hippocampal slices

Standard field excitatory postsynaptic potentials (fEPSP) were recorded in the CA1 region on acute mouse hippocampal slices as previously described (*26*). Briefly, 350-µm thick transverse slices from hippocampus of 6-8 week old C57BL/6x129 were incubated for > 90 min in artificial cerebrospinal fluid (aCSF) containing (in mM): 124 NaCl, 2 KCl, 2 $MgSO_4$, 1.25 NaH_2PO_4, 2.5 $CaCl_2$, 26 $NaHCO_3$, 10 D-glucose, pH 7.4, 310 mOsm, then were submerged beneath continuously perfused aCSF saturated with 95% O_2 and 5% CO_2 for stimulation at RT (~24 °C). For electrophysiology, standard fEPSP were recorded in the CA1 region of hippocampus. Briefly, stimulating electrode was placed in Schaffer collaterals to deliver test and conditioning stimuli, and borosilicate glass recording electrode filled with aCSF was positioned 200-300 µm from the stimulating electrode in stratum radiatum of CA1. C1q antibody or IgG isotype control was added 10 min before applying the vehicle aCSF control or S26C oligomers. 30 min later, high frequency stimulation was applied to induce LTP: two consecutive trains (1 s) of stimuli at 100 Hz separated by 20 s, a protocol that induces LTP lasting ~1.5 h in WT mice of this genetic background, were applied to the slices. The field potentials were amplified 100x using Axon Instruments 200B amplifer and digitized with Digidata 1322A. The

data were sampled at 10 kHz and filtered at 2 kHz. Traces were obtained by pClamp 9.2 and analyzed using the Clampfit 9.2.

Fluorescent in situ hybridization (FISH)

To confirm the expression of *C1qa*, FISH was performed on 10-µm slice of 4% PFA fixed brain. C1qa and NSE were used as double mRNA staining and Iba1 as immunostaining. C1qa and NSE anti-sense RNA was made and labeled by Cyanine and Fluorescein, respectively, with a RNA labeling kit from Roche. C1qa was synthesized from pCMV SPORT6 C1qa plasmid from Open Biosystems reference MMM1013-63584. A 500bp probe was designed with the following primers GGCATCCGGACTGGTATCC as forward and GTAAATGCGACCCTTTGCG as reverse. DNA was then digested using SalI and transcripted with T7 Promoter. The RNA probes were incubated 1 h at 64°C, and then detected with an antibody against the labeling from Roche. This immunoreaction was amplified with a TSA staining Kit from PerkinElmer. A Rabbit anti Iba1 was used to label the microglia and was detected with a Donkey anti Rabbit 647. The result was imaged and analyzed on a fluorescent microscope Zeiss AX10.

Statistical analysis

PRISM (Graphpad Software (Prism Version 5.0b)) was used to perform Student's *t*-test and analysis of variance (ANOVA), as appropriate. In order to control for multiple comparisons, we used Bonferroni's post-hoc testing procedure. In order to remove inter-day and inter-experiment variability, each transgenic animal or animal treated with Aβ was paired with its respective control and the analysis was performed on the normalized evaluation of the animal with respect to its respective control. For the normalized outcomes, the results are reported based on a one-sample *t*-test with null hypothesis set to 100.

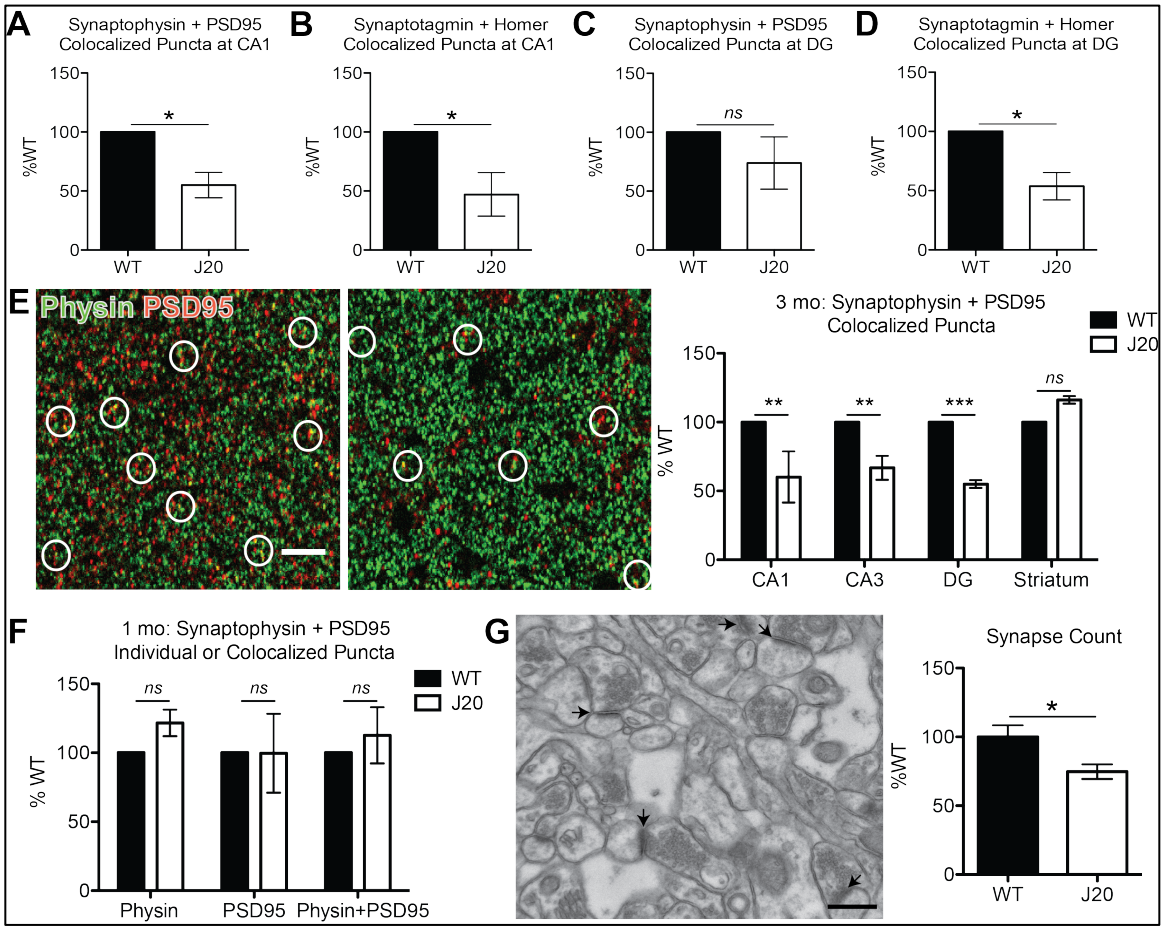

Fig. S1.

Early synapse loss in pre-plaque 3 mo J20 hippocampus. (**A-D**) Quantification of colocalization or apposition of pre- and postsynaptic markers using Imaris on super-resolution SIM images of hippocampus immunostained with synaptophysin and PSD95 (**A** and **C**) or synaptotagmin and homer (**B** and **D**) at the CA1 stratum radiatum (**A** and **B**) or dentate gyrus (**C** and **D**) show decreased synapse numbers in J20 mice compared to their WT littermate controls. (**E**) Loss of synapses in 3 mo J20 hippocampus as determined by quantification of colocalized pre- and postsynaptic puncta on confocal images. J20 striatum does not display such synapse loss compared to WT striatum (rightmost panel). (**F**) Normal synapse number in 1 mo J20 hippocampus. Quantification of synaptic puncta or their colocalization of high-resolution confocal images indicates similar levels of synapses in 1 mo J20 to their WT littermates in stratum radiatum (CA1). (**G**) Representative electron microscopy (EM) image of 3 mo CA1 stratum radiatum. Arrows indicate synapses, defined as an electron dense post-synaptic density areas juxtaposed to presynaptic terminals filled with synaptic vesicles. Synapse quantification of EM images show a significant reduction in J20 mice vs. WT. Scale bar = 0.5 (**G**) or 5 (**E**) µm. Means ± SEM, n = 3-4 mice per genotype. *$P < 0.05$, **$P < 0.01$, ***$P < 0.001$ using t-test (**A** to **D** and **G**) or two-way ANOVA followed by Bonferroni posttest (**E** and **F**).

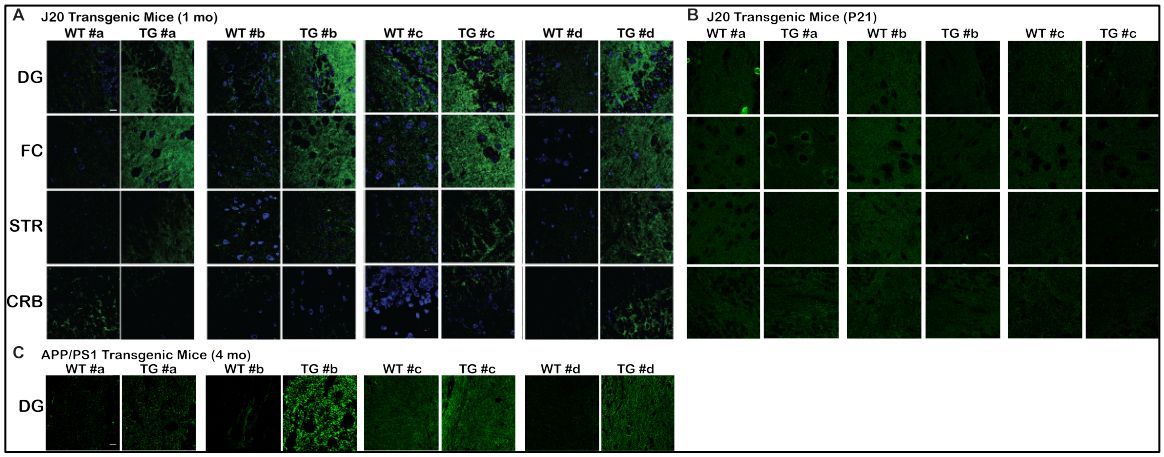

Fig. S2.

C1q is specifically increased in areas vulnerable to synapse loss in AD models. (**A**) High-resolution confocal imaging on 1 mo J20 and WT sex-matched littermates shows an early and region-specific increased levels of C1q (green) in the dentate gyrus (DG) and prefrontal cortex (FC), but not in striatum (STR) or cerebellum (CRB). (**B**) Similar levels of C1q were observed in P21 J20 brain vs. WT littermates, in contrast to the region-specific elevation of C1q observed at 1 mo (**A**). (**C**) 4 mo APP/PS1 mice have higher levels of C1q deposited in their dentate gyrus vs. their WT littermates. C1q (green), DAPI (blue). Scale bar = 10 μm. *n* = 3-4 mice per genotype.

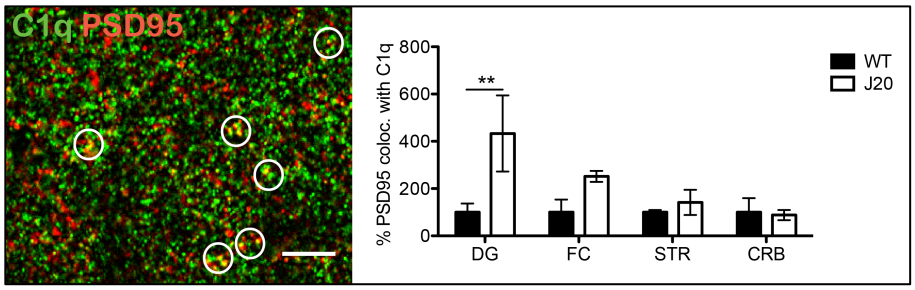

Fig. S3.

More synapses are found deposited with C1q in the vulnerable brain regions. As in SIM (see **Fig. 1**), high-resolution confocal imaging shows some PSD95 (red) to colocalize with C1q (green) in the 1 mo J20 dentate gyrus. Quantification using ImageJ shows that % PSD95 found colocalized with C1q is significantly higher in the J20 dentate gyrus and frontal cortex vs. controls. Scale bar = 5 μm. Means ± SEM; n = 3-4 mice per genotype. $^{**}P < 0.01$ using two-way ANOVA followed by Bonferroni posttest.

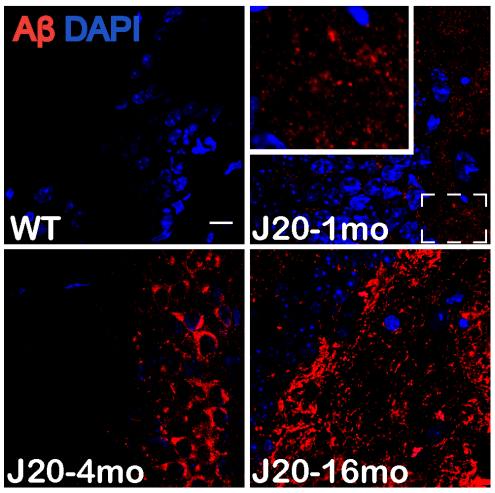

Fig. S4.

Aβ is deposited as early as 1 mo in J20 hippocampus. Representative high-resolution confocal images showing deposition of human-specific Aβ using 3D6 (red) in dentate gyrus of WT or 1 mo, 4 mo and 16 mo J20 mice. Scale bar = 5 μm. Zoomed inset demonstrates punctate Aβ staining in 1 mo J20 hippocampus.

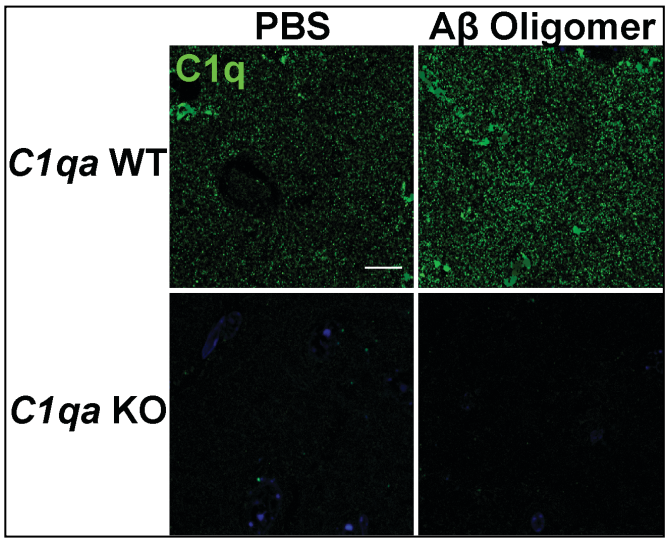

Fig. S5.

Oligomeric Aβ increases C1q protein deposition in WT mice. Synaptotoxic Aβ oligomers significantly upregulate C1q (green) immunoreactivity in the contralateral hippocampus of WT mice within 72 h of ICV injection. Scale bar = 10 μm.

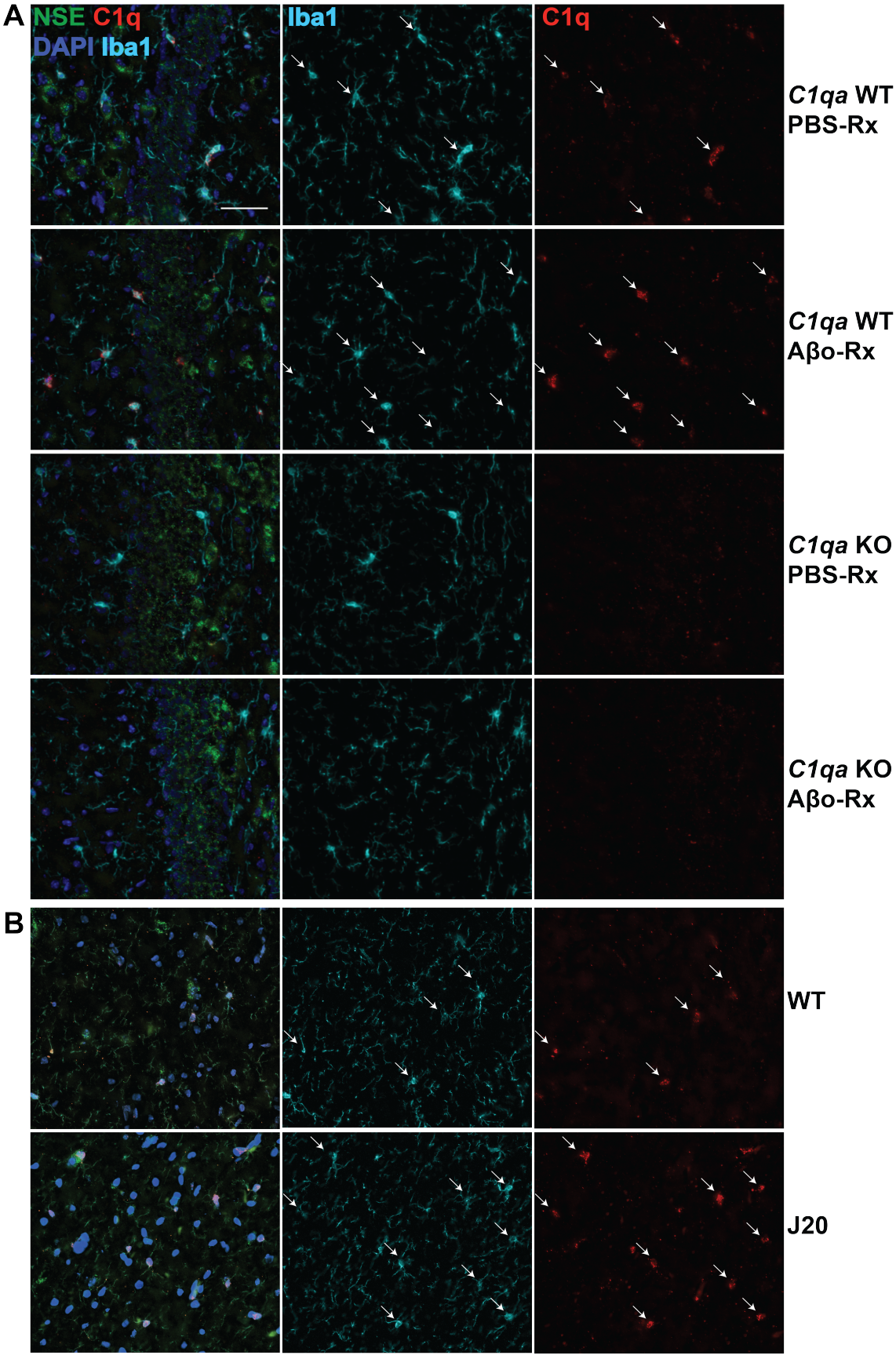
A
NSE C1q
DAPI Iba1
Iba1
C1q
C1qa WT
PBS-Rx
C1qa WT
Aβo-Rx
C1qa KO
PBS-Rx
C1qa KO
Aβo-Rx
B
WT
J20

Fig. S6.

Microglial *C1qa* is increased in hippocampi of J20 mice and in Aβ oligomer-treated WT mice. Fluorescent *in situ* hybridization (FISH) shows upregulation of microglial *C1qa* mRNA levels in contralateral hippocampus of WT mice injected with Aβ oligomers vs. PBS (two upper panels) (**A**) and J20 hippocampus vs. WT littermate controls (**B**). Arrows indicate examples of *C1qa* mRNA (red) expression patterns in Iba1-positive microglia (cyan) vs. NSE-positive neurons (green). Images of contralateral hippocampi of *C1qa* KO mice injected with PBS or Aβ oligomers are shown as controls (two bottom panels of **A**). Representative images of n = 3-4 mice per treatment group per genotype. Scale bar = 50 μm.

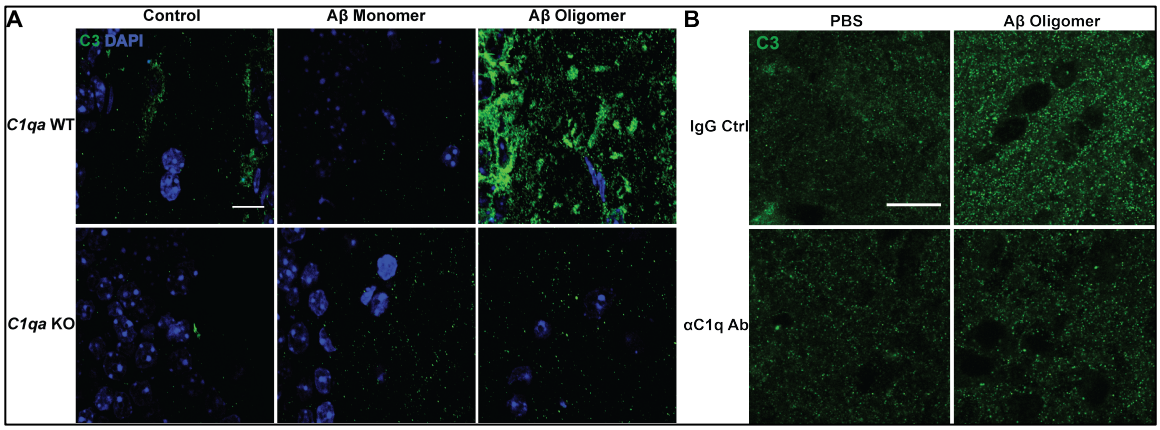

Fig. S7.

C3 activation in AD-like mouse brains is downstream of C1q. (**A**) Synaptotoxic Aβ oligomers, but not the monomers, significantly upregulated C3 (green) within 18 h of ICV injection in the contralateral hippocampus of WT mice; however, this effect was diminished in the *C1qa* KO mice. (**B**) Compared to PBS control, the synaptotoxic Aβ oligomers increased C3 immunoreactivity in contralateral hippocampus of WT mice co-injected with IgG isotype control (upper panels); however, they markedly failed to do so in mice co-injected with the ANX-M1 anti-C1q antibody (lower panels). Scale bar = 10 (**A**) or 15 (**B**) μm. Representative images of $n = 3$ mice per treatment group per genotype.

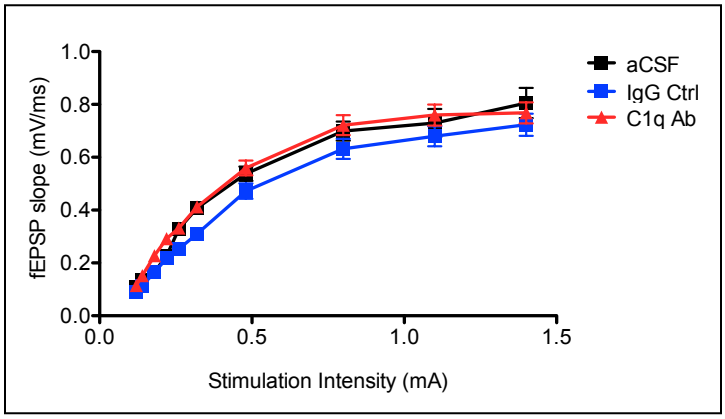

Fig. S8.

ANX-M1 anti-C1q antibody does not alter the basal neurotransmission in acute mouse hippocampal slices. The input/output curves were recorded on 30 min after aCSF vehicle (black), IgG isotype control (blue) or the anti-C1q antibody (red) was added to the perfusion buffer. Means ± SEM; *n* = 6-11 slices per group.

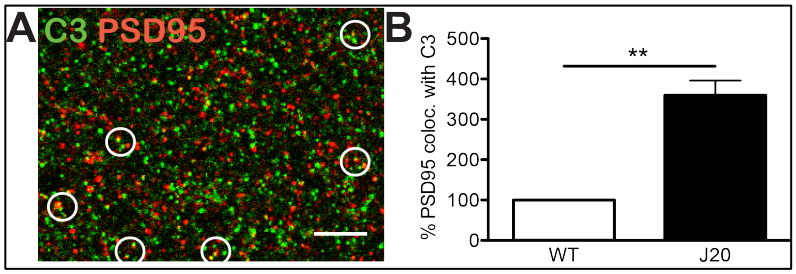

Fig. S9.

C3 is localized onto PSD95 in J20 hippocampus. (**A**) Representative confocal image showing colocalization of C3 (green) and PSD95 (red). Scale bar = 5 μm. (**B**) Quantification using ImageJ shows that % PSD95 found colocalized with C3 is significantly higher in the dentate gyrus of 1 mo J20 mice vs. WT littermates, similar to this colocalization in APP/PS1 mice (see **Fig. 3D**). Mean ± SEM; n = 4 mice per genotype. $^{**}P < 0.01$ using one-sample two-tailed t-test.

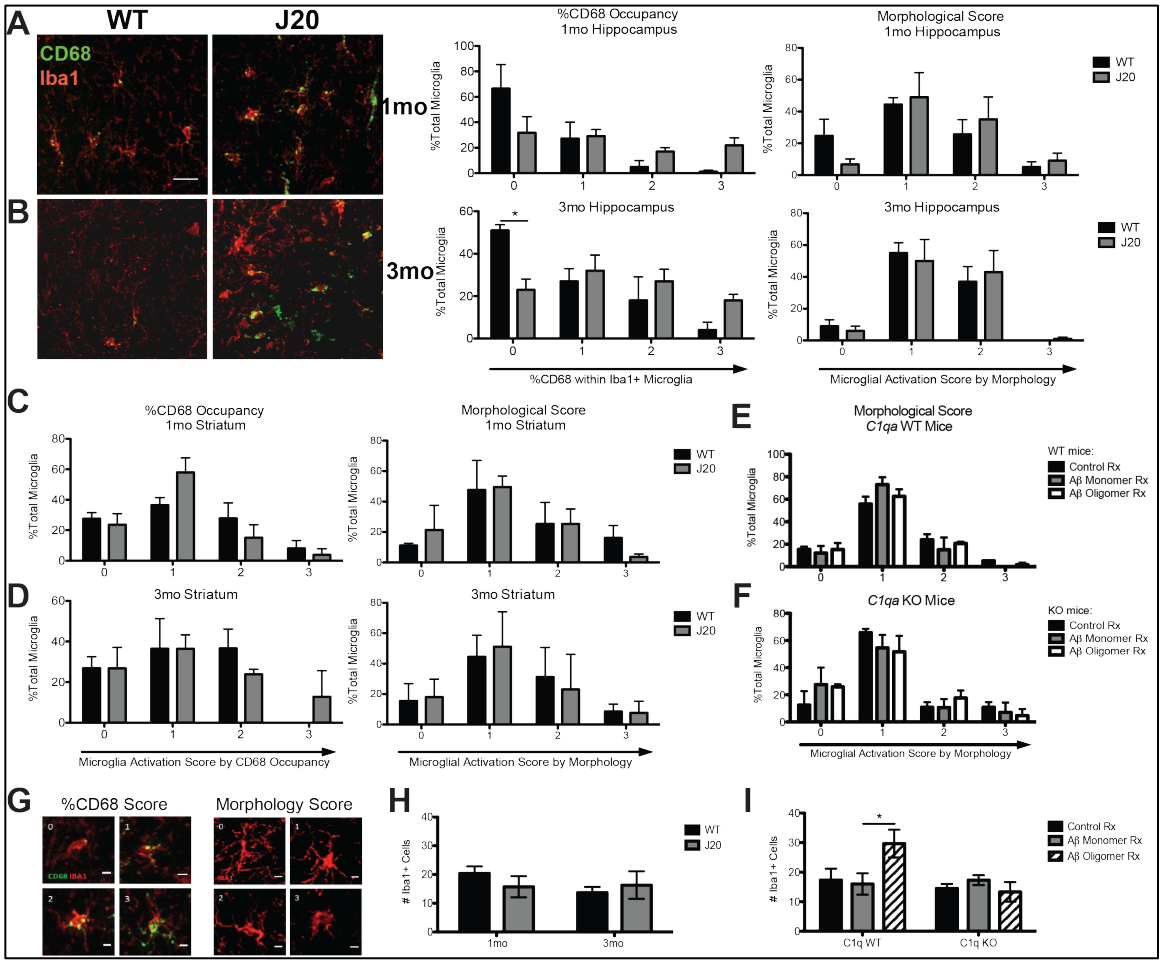

Fig. S10.

More phagocytic microglia reside in hippocampus of pre-plaque J20 mice. To characterize microglial phagocytic activity, we examined CD68 (green) occupancy within Iba1-positive (red) microglia and morphology of the Iba1-positive cell following a similar protocol in Schafer et al. (*6*). For microglial levels of CD68, a glycoprotein that localizes to lysosomes and endosomes, CD68 levels were quantified on a scale from 0 to 3. A score of 0 signified no/scarce expression; 1 for punctate expression; and 2 (roughly one-third to two-thirds occupancy) or 3 (greater than two-thirds occupancy) for punctate expression covering an entire cell or aggregated expression (see **G**). For morphology, a score of 0 was given to microglia with thin, long processes with multiple branches; 1 for microglia with thicker processes with branches; 2 for microglia with thick, retracted processes with few branches; and 3 for round microglia without processes (see **G**). Each microglial cell in an image received CD68 and morphology scores, and the percent of microglia receiving a particular score was calculated for each image (number receiving score/total number of microglia x 100). These percentages were averaged for each score for each genotype (**A-D**) or treatment (**E** and **F**, also see **Figs. 2C** and **2D**). All analysis was performed blinded. (**A-D**) Microglia in CA2 hippocampus (**A** and **B**) or striatum (**C** and **D**) of 1 mo (upper panels) or 3 mo (lower panels) WT and J20 mice were examined as described above. There is a trend toward increased lysosomal activity, *i.e.*, more %

microglia in 1 mo J20 hippocampus have CD68 score of 2 and 3, with minimal difference in morphology (**A**). Increased CD68 burden, with little difference in morphology, in microglia of 3 mo J20 mice. There was a significantly less % microglia that have negligible CD68 occupancy in 3 mo hippocampus compared to WT controls (**B**). There was no difference in either CD68 occupancy or morphological score in microglia of J20 and WT striatum at either 1 (**C**) or 3 mo (**D**). (**E** and **F**) In contrast to increase in CD68 occupancy, there was no appreciable difference in microglial morphology of WT mice injected with Aβ oligomers (**E**) (see **Fig. 2C**). There was no appreciable difference in microglial morphology of *C1qa* KO mice injected with Aβ (**F**). (**H** and **I**) Quantification of Iba1-positive microglia in J20 and WT CA2 hippocampus at 1 and 3 mo (**H**) and in contralateral CA2 hippocampus of WT and *C1qa* KO mice challenged with control (no injection or PBS), Aβ monomers, or oligomers (**I**) shows that there are no appreciable changes in number of microglia, except in WT hippocampus challenged with oAβ. Means ± SEM; $n = 3$ mice per genotype or per treatment per genotype. $^*P < 0.05$ using two-way ANOVA followed by Bonferroni posttest. Scale bar = 5 (**G**) or 20 μm (**A** and **B**).

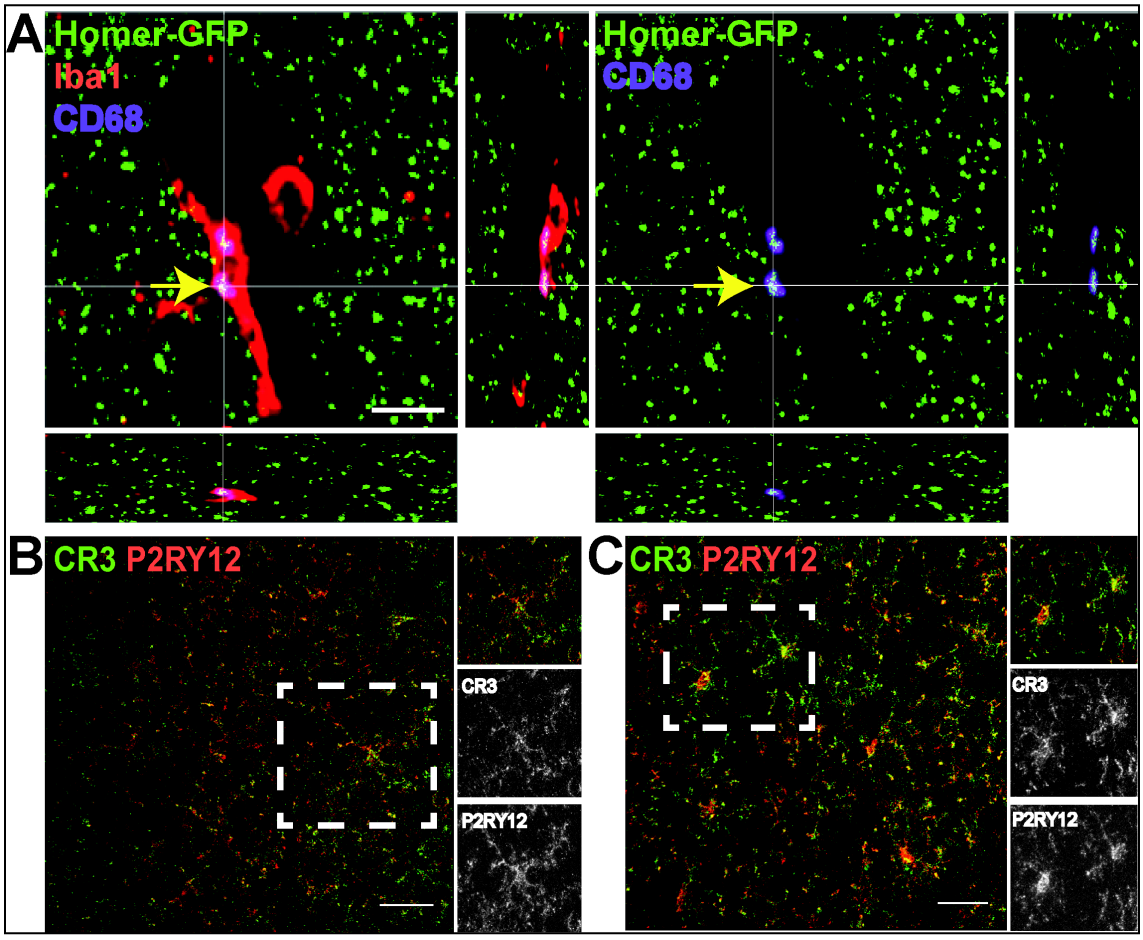

Fig. S11.

Engulfed synapses in resident microglia localize to lysosomes. (**A**) Engulfed synapses were often found localized to internal lysosomal compartments. An orthogonal view of a representative high-resolution confocal image shows colocalization of Homer-GFP with CD68-immunoreactive lysosomal compartment (purple) of an Iba1-positive microglia (red). (**B** and **C**) CR3-positive cells in pre-plaque brains of AD mouse models are of resident origin. Representative views of hippocampi of 3 mo J20 transgenic mice (**B**) and 3 mo WT mice injected with Aβ oligomers (**C**) show all CR3-positive cells (green) to be co-stained with P2RY12 (red), a marker for resident microglia (*22*). Representative images of 3 pairs of mice per genotype per treatment group. Scale bar = 5 (**B**) or 20 (**C**, **D**) μm.

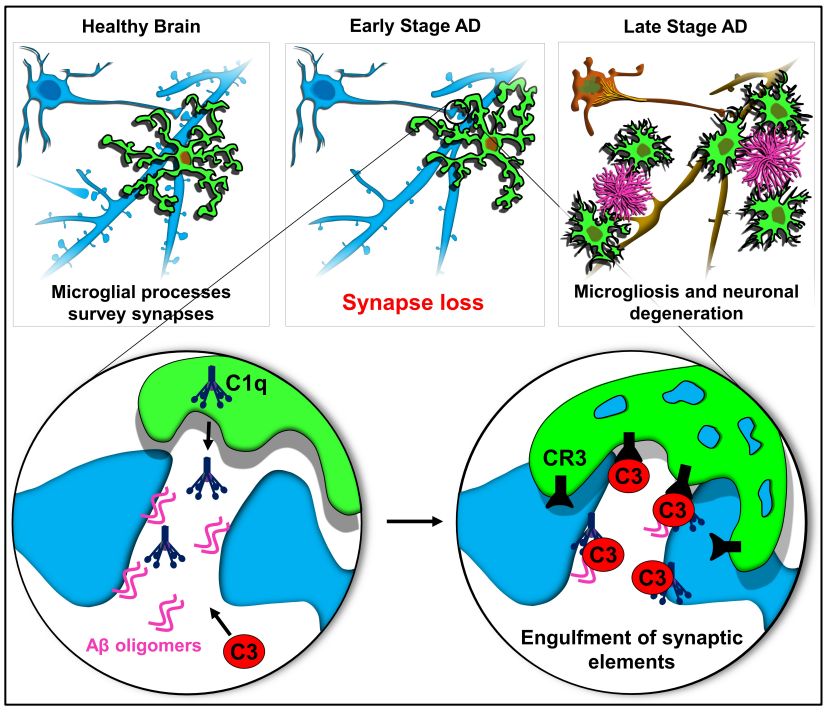

Fig. S12.
Microglia engulf synaptic elements via complement signaling in pre-plaque AD brains. Synapse loss is an early hallmark of AD pathology, thought to be initiated by soluble Aβ oligomers. However, mechanisms underlying synapse loss remain elusive. Here, we show that the soluble Aβ oligomers activate a developmental synapse pruning mechanism to mediate synapse loss. Local activation of complement (C1q and C3) at vulnerable synapses by oligomeric Aβ (oAβ) leads to microglial engulfment of these synapses through C3/CR3 signaling. Inhibition of the complement pathway or microglial engulfment of synaptic material using genetic and/or antibody-mediated methods leads to rescue of oAβ-induced synapse loss and dysfunction. Taken together, we identify a novel role of microglia and the classical complement cascade in synapse loss in AD models. This role of the immune pathway is distinct from the well-established microgliosis and activation of the complement cascade in plaque-enriched AD brains in later stages of the disease pathogenesis. Figure adapted from Hong et al., Current Opinion in Neurobiology 2016 (*1*).